$^1B_2(^1\Sigma_u^+)$ excited state decay dynamics in CS$_2$

Dave Townsend and Helmut Satzger
Steacie Institute for Molecular Sciences, National Research Council of Canada, Ottawa, Ontario K1A 0R6, Canada

Tine Ejdrup
Department of Chemistry, University of Aarhus, 8000 Arhus C, Denmark

Anthony M. D. Lee
Steacie Institute for Molecular Sciences, National Research Council of Canada, Ottawa, Ontario K1A 0R6, Canada and Department of Chemistry, Queen's University, Kingston, Ontario K7L 3N6, Canada

Henrik Stapelfeldt
Department of Chemistry, University of Aarhus, 8000 Arhus C, Denmark

Albert Stolow
Steacie Institute for Molecular Sciences, National Research Council of Canada, Ottawa, Ontario K1A 0R6, Canada Department of Physics, Queen's University, Kingston, Ontario K7L 3N6, Canada

The authors report time resolved photoelectron spectra of the $^1B_2(^1\Sigma_u^+)$ state of CS$_2$ at pump wavelengths in the region of 200 nm. In contrast to previous studies, the authors find that the predissociation dynamics is not well described by a single exponential decay. Biexponential modeling of the authors' data reveals a rapid decay pathway ($\tau < 50$ fs), in addition to a longer lived channel ($\tau \sim 350-650$ fs) that displays a marked change in apparent lifetime when the polarization of the pump laser is rotated with respect to that of the probe. Since the initially populated $^1B_2(^1\Sigma_u^+)$ state may decay to form either S(^1D) or S(^3P) products (the latter produced via a spin-orbit induced crossing from a singlet to a triplet electronic surface), this lifetime observation may be rationalized in terms of changes in the *relative* ionization cross section of these singlet and triplet states of CS$_2$ as a function of laser polarization geometry. The experimentally observed lifetime of the longer lived channel is therefore a superposition of these two pathways, both of which decay on very similar time scales. © *2006 American Institute of Physics.* [DOI: 10.1063/1.2403137]

I. INTRODUCTION

In the past three decades there has been considerable effort invested in developing a more detailed understanding of the nonadiabatic dynamics that plays a role in the photo-dissociation of the CS$_2$ molecule following excitation in the 185–230 nm region. This strong absorption band is attributed to a parallel electronic transition from the linear $\tilde{X}(^1\Sigma_g^+)$ ground state to a singlet excited state, conventionally labeled as $^1\Sigma_u^+$ within the $D_{\infty h}$ point group, and which then correlates with $^1B_2$ as the molecule bends and descends to C_{2v} symmetry. To reflect this, the state is usually denoted as $^1B_2(^1\Sigma_u^+)$ (see Ref. 1); however, it is also often referred to simply as S_3. Specifically, the optical excitation involves the promotion of an electron from a $2\pi_g$ molecular orbital, predominantly localized on the terminal sulfur atoms and largely S–C nonbonding in character, to a $3\pi_u^*$ antibonding orbital predominantly localized on the central carbon atom.[2–4] This brings about an increase in the C–S bond length from 1.55 to 1.66 Å and a reduction in the S–C–S bond angle from 180° to around 153°.[5] The initially prepared linear excited state is strongly bound along the antisymmetric SC–S stretching coordinate, ν_3'. Outside the Franck-Condon region, the $^1\Sigma_u^+$ potential surface is crossed by several purely dissociative electronic states, and one of these ($^1\Pi_g$) becomes

$^1A_2 + {}^1B_2$ in character as the molecule begins to bend (Renner-Teller splitting). This results in an avoided crossing between the $^1B_2$ component and the initially prepared excited state (which is now also described as $^1B_2$) and enables the CS$_2$ molecule to predissociate into CS($X\,^1\Sigma^+$)+S($^1D_2$) products. This is illustrated schematically in Fig. 1. The first detailed investigation into the dissociation dynamics of this system under collision-free conditions was carried out at 193.3 nm by Yang *et al.*[6] In addition to observing S($^1D_2$) atoms (the singlet channel), these authors also reported a significant yield of S(^3P_J) fragments (the triplet channel), and this second pathway has been attributed to spin-orbit coupling mediating a crossing to the dissociative $^3\Pi_g(^3A_2 + {}^3B_2)$ triplet state, as will be discussed in more detail later.

Due to the shallow slope of the dissociative $^1B_2$ potential surface derived from the $^1\Sigma_u^+$ state, the predissociation lifetime is sufficiently long to enable the observation of discrete vibrational bands in the CS$_2$ absorption spectrum. The $^1B_2(^1\Sigma_u^+)$ state is bound along the coordinates describing both the symmetric stretch, ν_1', and the bending vibration, ν_2', and numerous researchers have reported progressions based upon excitation of various combinations of these two modes.[5,7–14] However, attempts to produce a fully quantitative assignment of all the features within this absorption band have been

125, 234302-1
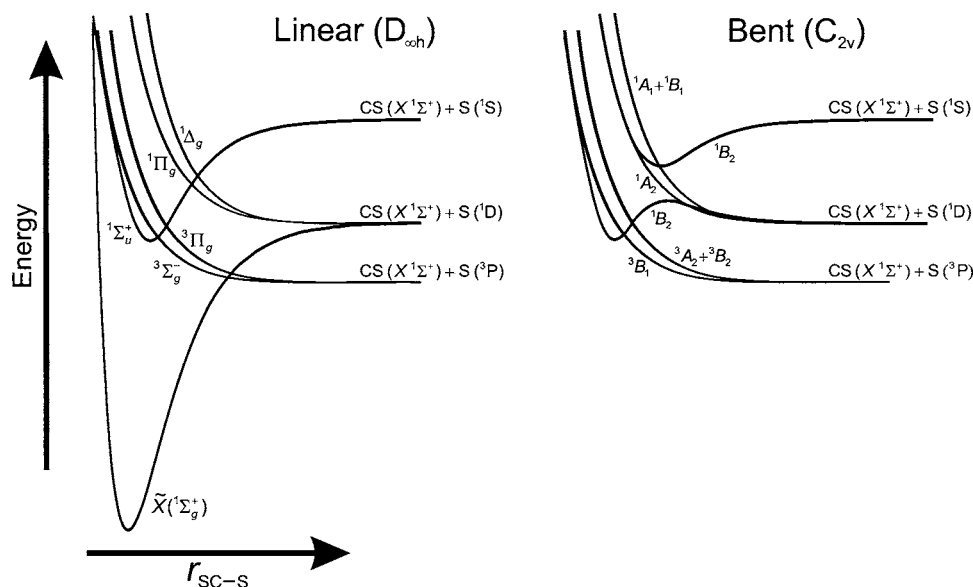
FIG. 1. Schematic overview of the potential energy curves of CS_2 in the 185–230 nm absorption region along the antisymmetric stretching coordinate, ν_3, in linear and bent configurations.

complicated over the years by a number of factors: (1) Poor Franck-Condon overlap in the low energy region of the spectrum prevented unambiguous determination of the $^1B_2(^1\Sigma_u^+)$ electronic origin (although a value close to 46 248 cm^{-1} now seems to be accepted[5,11,13]). (2) The near degeneracy of the symmetric stretching and bending modes induces significant perturbations into the spectrum, particularly in both the red and blue wings of the absorption band. The irregular vibrational progressions observed as a consequence of these interactions are therefore not well described by a simple harmonic model. Detailed analysis is further complicated by the large number of hot band transitions that appear in the room temperature spectrum. (3) At higher energies, the rapidly increasing rate of predissociation broadens the absorption lines to a large extent, obscuring many of the spectral features.[8]

In spite of these inherent difficulties, a considerable amount of detailed information concerning the $^1B_2(^1\Sigma_u^+)$ $\leftarrow \tilde{X}\,^1\Sigma_g^+$ transition is now known. In an attempt to simplify the (unassigned) high resolution gas cell spectra reported by Douglas and Zanon[5] between 43 300 and 48 500 cm^{-1}, Vaida and co-workers employed molecular beam methods in the study of absorption to the $^1B_2(^1\Sigma_u^+)$ state in the 47 750–53 200 cm^{-1} region.[9,10] By eliminating many of the hot band transitions and narrowing the rotational manifold associated with each observed vibrational line, vibrational frequencies were assigned to the symmetric stretch, ν_1'=392 cm^{-1}, and bending, ν_2'=426 cm^{-1}, modes based upon a series of regular progressions containing contributions from these two moieties in a region near the Franck-Condon maximum (49 000–51 000 cm^{-1}). Although it was possible to determine the *relative* weighting of the ν_1' and ν_2' components for each observed absorption line, definitive assignment of vibrational quantum numbers was not possible at that time owing to the uncertainty in the position of the electronic origin, as mentioned previously. Additionally, by looking at changes in the A rotational constant (associated with the K quantum number) in the bent $^1B_2(^1\Sigma_u^+)$ state as a function of increasing excitation energy (in instances where some hot bands were still present), it was concluded that the potential

barrier preventing CS_2 from assuming a quasilinear geometry was overcome at around 49 000 cm^{-1} above the ground state origin. A more recent study by Arendt and Butler[12] used emission spectroscopy between 48 500 and 51 000 cm^{-1} to determine the position of this "barrier to linearity" on the basis of the propensity to populate stretching versus bending vibrations in a jet cooled beam across this region, producing a revised estimate of between 49 312 and 49 662 cm^{-1}.

Work by Donaldson[11] using a room temperature sample of CS_2 in conjunction with $(1+1)$ and $(2+2)$ resonantly enhanced multiphoton ionization (REMPI) in the 45 500–48 100 cm^{-1} region largely confirmed many of the assertions of Vaida and co-workers, concluding that below the barrier to linearity the bending vibration was excited more readily than the symmetric stretch, and assigning ν_1'=400 cm^{-1} and ν_2'=429 cm^{-1}. This work also concluded that the electronic origin was at 46 247 cm^{-1} and, based upon the differing selection rules for one- and two-photon excitations, assigned a weak transition to the lowest lying vibration in the asymmetric stretching mode, ν_3', at a frequency of 1567 cm^{-1}. This low energy region of the absorption spectrum was subsequently reinvestigated by Beatty et al.[13] using $(1+1)$ REMPI in conjunction with jet cooled beams of both $^{12}C^{32}S_2$ and $^{12}C^{34}S^{32}S$. Transitions arising from several different vibrational levels in the electronic ground state were categorized and the line positions found to be in reasonably good agreement with those previously reported by Douglas and Zanon[5] and by Donaldson[11] [including an assignment of the $^1B_2(^1\Sigma_u^+)$ state origin at 46 248.7 cm^{-1}]. In keeping with the assertions of the original Douglas and Zanon study, it was concluded that the line positions were simply too perturbed to permit a quantitative vibrational assignment and that a normal mode description of the $^1B_2(^1\Sigma_u^+)$ state vibrational motions is not applicable. On the basis of the spectral linewidths, lifetimes were determined for each absorption line. Transitions starting from the zero point level of the electronic ground state (denoted Σ_0, see Ref. 15) exhibited a fall in lifetime from 3.7 to 1.0 ps with increasing excitation energy, although this trend is somewhat irregular and addi-

tionally has a pronounced "spike" at around 47 500 cm^{-1} (210 nm). Hot band transitions originating from $\nu_2''=1$ (labeled Π_1) were observed to exhibit lifetimes in the 1.8–0.4 ps range. The generally faster predissociation rate for hot band versus fundamental transitions was attributed to the selection rules governing transitions from levels with different angular momenta in the linear ground state (as indicated by the Σ and Π labels) to the bent $^1B_2(^1\Sigma_u^+)$ state (see Ref. 16). This subsequently influences the coupling rate to nearby dissociative continua, as will be discussed in more detail shortly. Lifetimes quoted for the Σ_0 transitions were in good agreement with those determined from room temperature resonance Raman depolarization measurements at 208 and 212 nm by Li and Meyers,[17] although were somewhat lower than those reported by Liou *et al.* at 210 nm[18] and by Hara and Phillips,[8] who used fluorescence quantum yield measurements in a gas cell to infer lifetimes of 1.1–9.0 ps in the 200–215 nm region.

In addition to the studies outlined above detailing the spectroscopic features of the CS$_2$ $^1B_2(^1\Sigma_u^+)$ absorption, a great deal of work characterizing the nature of the photofragments produced following the dissociation of this excited state has also been undertaken. The majority of these investigations have been carried out at the (experimentally convenient) argon fluoride excimer wavelength of 193.3 nm ($\sim$51 730 cm^{-1}). As already briefly mentioned earlier in this section, two fragmentation pathways are observed:

$$\mathrm{CS_2}(\widetilde{X}\,^1\Sigma_g^+) \xrightarrow{h\nu} \mathrm{CS}(X\,^1\Sigma^+) + \mathrm{S}(^3P_J), \tag{1a}$$

$$\mathrm{CS_2}(\widetilde{X}\,^1\Sigma_g^+) \xrightarrow{h\nu} \mathrm{CS}(X\,^1\Sigma^+) + \mathrm{S}(^1D_2). \tag{1b}$$
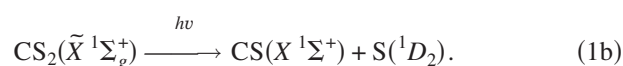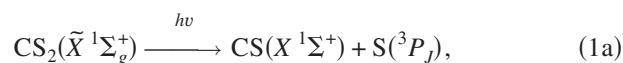
While there is largely a general consensus in the literature regarding the energy partitioning within the CS fragment [significant rotational excitation in both channels, with $\nu=0$–4 and $\nu_{max}=3$ for S($^1D_2$), $\nu=0$–12 and $\nu_{max}\sim7$–10 for S(^3P_J) (Refs. 6 and 19–25)], the relative contribution of the singlet and triplet pathways has been the subject of considerable controversy over the years. Branching ratios ranging from S(^3P_J)/S($^1D_2$)=0.25 to 6.0 have been previously reported,[6,20,25–28] with much of the discrepancy originating from problems associated with the secondary photolysis of the CS product at high laser intensities. Measurements made by Waller and Hepburn using vacuum ultraviolet laser-induced fluorescence (VUV-LIF) to probe the S-atom photoproducts appeared to finally establish a value of S(^3P_J)/S($^1D_2$)=2.8±0.3 as the correct one,[21] as this observation was confirmed in subsequent work using time-of-flight mass spectrometry[22] and vuv ionization.[23] Two recent ion imaging measurements from Kitsopoulos *et al.*, S(^3P_J)/S($^1D_2$)=1.5±0.4,[24] and Xu *et al.*, S(^3P_J)/S($^1D_2$)=1.6±0.3,[29] have once again brought this value into question, however [although it is interesting to note that the values quoted for the more specific S($^3P_2$)/S($^1D_2$) ratio by Waller and Hepburn (1.96±0.17) and by Kitsopoulos *et al.* (1.9±0.2) are in good agreement].

A considerable degree of controversy also exists concerning the angular distributions of the S-atom fragments
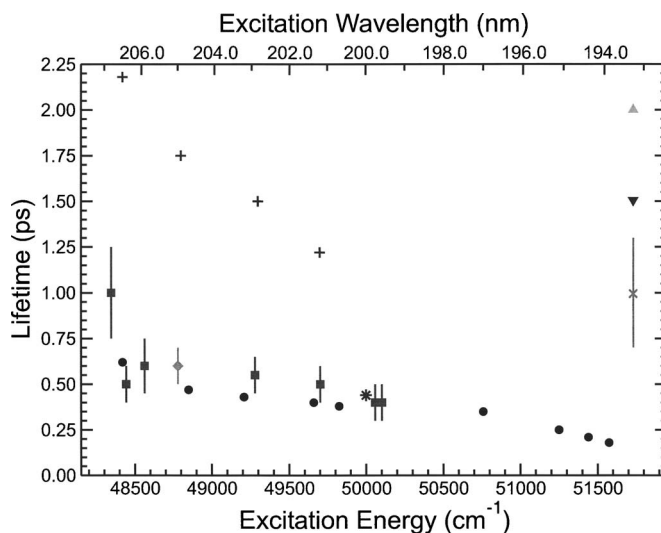
FIG. 2. Summary of lifetime measurements previously reported for the $^1\Sigma_u^+(^1B_2)$ state of CS$_2$ in the 48 250–51 750 cm^{-1} region using various techniques. (+) Fluorescence yield (Ref. 8), ($\times$, $\blacktriangle$, $\blacktriangledown$) photofragment angular distribution (Refs. 6, 21, and 30), ($*$) resonance Raman depolarization (Refs. 17, 50, and 51), ($\blacksquare$) PHOFEX linewidth (Ref. 34) and ($\blacklozenge$, $\bullet$) femtosecond REMPI (Refs. 35 and 36). For a summary of reported lifetimes below 48 250 cm^{-1} see Fig. 5 of Ref. 34 and Table I of Ref. 13.

produced at 193.3 nm. Explicit values for the recoil anisotropy parameter β have been reported between 0.2 and 1.9 for S($^1D_2$) and between 0.2 and 1.0 for S(^3P_J) without any consistent trend in the relative degree of anisotropy in the two channels even being apparent from measurement to measurement.[21,24,29,30] Reflecting this uncertainty, in cases where the angular distribution has been used to infer the $^1B_2(^1\Sigma_u^+)$ state lifetime, values in the range of 0.6–2.0 ps have been quoted,[6,21,30] as summarized in Fig. 2.

A detailed discussion concerning the large number of discrepancies in the various experimental results quoted in the literature for the photodissociation of CS$_2$ at 193.3 nm is beyond the scope of this Communication. Even under collision-free conditions, problems introduced by such factors as laser induced secondary photolysis of CS fragments and uncertainties in the relative oscillator strengths and ionization cross sections required to interpret the various detection schemes that have been employed mean that a definitive description of the photodissociation at 193.3 nm is yet to be presented.

Only a handful of studies probing the photodissociation products of the $^1B_2(^1\Sigma_u^+)$ state at photolysis wavelengths other than 193.3 nm have currently been reported. Liou *et al.*[18] observed vibrational excitation up to $\nu=6$ in the CS ($X\,^1\Sigma^+$) fragment at 210 nm and, by stimulated emission pumping within the ground state, found the lifetime of a given final excited state to be highly dependent on the initially populated vibrational level.[31] At around 215 nm the predissociation rate was observed to be largely (although not completely) independent of rotational excitation.[32] Starrs *et al.* recorded photofragment excitation (PHOFEX) spectra at photolysis energies around 47 600–48 100 cm^{-1} (210–208 nm), probing both the S($^3P_0$, $^3P_1$, $^3P_2$) and S($^1D_2$) atoms that were produced.[33] Transitions originating from $\nu_2''=0$ in the ground state (labeled Σ_0 and correlating with K'

=0 in the bent excited state) were found to show a much higher propensity for forming $S(^3P_2)$ over $S(^3P_1)$, $S(^3P_0)$, and $S(^1D_2)$ fragments. This preferential population of the $S(^3P_2)$ channel appeared to be suppressed in Π_1 hot band transitions [originating from $\nu_2''=1$ and correlated with $K'=1$ in $^1\Sigma_u^+(^1B_2)$], while the production of $S(^1D_2)$ was significantly augmented. This work was then expanded upon considerably in a follow-up publication by Mank *et al.*, who reported $S(^3P_0, {}^3P_1, {}^3P_2)$ and $S(^1D_2)$ PHOFEX spectra right across the 46 600–50 500 cm^{-1} (214–198 nm) region.[34] With increasing excitation energy, $^1B_2(^1\Sigma_u^+)$ state lifetimes of 1.5–0.3 and 1.2–0.18 ps were deduced (from an analysis of peak linewidths) for the observed series of Σ_0 and Π_1 transitions, respectively. For energies above 48 250 cm^{-1} (the region relevant to the present study) these values are plotted in Fig. 2. At energies below 48 550 cm^{-1} (wavelengths above 206 nm) significant differences in the relative line intensities in the $S(^3P_2)$ and $S(^1D_2)$ spectra were once again observed. $S(^3P_2)/S(^1D_2)$ branching ratios were seen to vary between values >12 and as low as 1.1, depending on the nature and position of the transition being excited, with the highest values being reported for Σ_0 transitions towards longer wavelengths. The enhanced production of $S(^1D_2)$ fragments for the $K'=1$ vs $K'=0$ levels of the excited state was attributed to the onset of a more effective coupling (such as a Coriolis interaction) between the bound molecular coordinates (ν_1', ν_2') and the dissociative antisymmetric stretch, ν_3'. Additionally, coupling to triplet surfaces asymptotically correlating with $S(^3P_2)$ fragments also appeared to be enhanced for $K'=1$, possibly indicating that the singlet-triplet coupling is displaced along the ν_3' coordinate. This coupling also increased in strength as the molecule assumed a quasilinear geometry in the $^1B_2(^1\Sigma_u^+)$ state at higher excitation energies. One final point of note in this study was the reported observation of a weak continuum background of S-atom products, present at all excitation wavelengths, upon which the resonant lines of the $^1B_2(^1\Sigma_u^+)$ state absorption were superimposed. This will be discussed in more detail later.

The various lifetime measurements summarized here up to this point have all been deduced from *indirect* measurements such as absorption linewidths or photofragment angular distributions. The first *direct* experimental observation of predissociation in the $^1B_2(^1\Sigma_u^+)$ state was made by Baronavski and Owrutsky using femtosecond pump-probe ion yield measurements.[35] Following excitation at 205 nm (48 780.5 cm^{-1}) they reported a lifetime of 600±100 fs, in good agreement with the values inferred by Mank *et al.* from linewidth measurements at similar photolysis energies.[34] A more expansive time resolved study was carried out by Farmanara *et al.*,[36] who studied the predissociation dynamics of CS_2 across the 194–207 nm region (51 550–48 300 cm^{-1}), observing lifetimes between 180 and 620 fs (at the red and blue limits of the study, respectively). An almost constant plateau in the lifetime (~400 fs) occurred at excitation energies around 50 000 cm^{-1} and was attributed to the geometry change associated with overcoming the barrier to linearity. Once again, these results are summarized in Fig. 2. Owing to the large [~120 cm^{-1} full width at half maximum (FWHM)] bandwidth inherently associated with the 130 fs pulses used

in this study, in some instances it was possible to simultaneously excite a pair of closely spaced levels in the $^1B_2(^1\Sigma_u^+)$ state (from the jet-cooled ground state), for example, the levels $(\nu_1'+1, \nu_2')$ and $(\nu_1', \nu_2'+1)$. In these cases it was found that distinct modulations were observed on top of the exponentially decaying CS_2^+ ion yield signal. This phenomenon was attributed to quantum beating between the coherently prepared vibrational bands. A "switching on" of this effect was even demonstrated in a warm sample of CS_2 excited at 206.5 nm, where the emergence of hot band transitions arising from $\nu_2''=1$ in the ground state induces a beating modulation in the pump-probe decay signal which is not seen in the vibrationally cold sample.

In this Communication we present a new investigation into the decay dynamics of the $^1B_2(^1\Sigma_u^+)$ state of CS_2 employing femtosecond time resolved photoelectron spectroscopy (TRPES). By directly observing the evolution of the excited state lifetime using different combinations of pump and probe laser polarization geometries, new insight into the coupling rates of the bending and stretching components of the vibrational motion with the dissociative continua may be determined. Additionally, by observing the dispersed spectrum of photoelectron energies, subtleties in the dynamics that may be obscured in "energy integrated" ion yield measurements may often be revealed, as has previously been well documented.[37–39]

II. EXPERIMENT

Our experimental setup employs a "magnetic bottle" photoelectron spectrometer which has previously been described in detail elsewhere.[40,41] Only the key points specific to this investigation will be outlined here. Briefly, approximately 300 Torr of helium was bubbled through a sample of liquid CS_2 (Fisher, 99.9%) held at −20 °C and then expanded through a 150 μm nozzle into a source chamber to create a continuous molecular beam. After traveling through a double skimmer arrangement and into a differentially pumped main chamber, this beam passed between the pole pieces of the magnetic bottle where it was intersected at 90° by two copropagating laser pulses. Both the pump beam ($\lambda_{\text{pump}} \sim 200$ nm) and probe beam ($\lambda_{\text{probe}} \sim 267$ nm) were produced from the output of a seeded Ti:sapphire regenerative amplifier (Positive Light, Spitfire) pumped by two 1 kHz Nd:YLF (yttrium lithium fluoride) lasers (Positive Light, Evolution). The seed beam (~800 nm) was provided by a Ti:sapphire oscillator (Spectra Physics, Tsunaimi) pumped by a Nd:YLF diode laser (Spectra Physics, Millennia). The tunable central frequency of the seed could be adjusted using an intracavity slit and set such that the final spectral output from the regenerative amplifier was centered between two closely spaced vibrational peaks in the $^1B_2(^1\Sigma_u^+) \leftarrow \tilde{X}\, {}^1\Sigma_g^+$ band of the CS_2 absorption spectrum. The pump beam was produced by generating the fourth harmonic of the regenerative amplifier output using a three-stage sum-frequency mixing scheme and was then attenuated to ~300 nJ. The probe beam was produced via third harmonic generation using a two-stage sum-frequency setup and was reduced to ~4 μJ. Rotation of the probe beam polarization relative to the pump

TABLE I. CS$_2$ transition frequencies, intensities, and vibrational assignments used in this work.

Transition frequency[a] (cm^{-1})	Relative intensity[a]	Assignment[a]	λ_{pump} (cm^{-1})	λ_{pump} (nm)
49 663	59	ν'_1+1, ν'_2	49 677	201.3
49 697	100	ν'_1, ν'_2+1		
50 055	81	ν'_1+2, ν'_2	50 075	199.7
510 097	93	ν'_1+1, ν'_2+1		

[a]Reference 9.

was achieved using a Berek compensator (New Focus), and the temporal delay between the two pulses was precisely controlled using a motorized linear translation stage (Newport, ILS250PP) and driver (Newport, ESP300) under personal computer (PC) control. The two beams were combined on a dichroic mirror and focused into the interaction region using a concave spherical aluminum mirror (f=50 cm). Photoelectrons were detected by a microchanel plate (MCP) detector positioned at the end of the magnetic bottle flight tube. The output signals from the MCP were then amplified (10 × Phillips Scientific 6950) before being digitized and processed by a PC. Using CaF$_2$ Brewster angle prism compressors for each laser beam, it was possible to obtain a pump-probe cross correlation width of ~160 fs. This measurement was obtained directly from nonresonant, two-color multiphoton ionization of both NO and NH$_3$, and these data were also used to provide time of flight to energy calibration of the magnetic bottle. The spectral bandwidth (FWHM) of both the pump and the probe pulses was determined to be ~400 cm^{-1}. A typical data collection run consisted of stepping the translation stage repeatedly between pump-probe delays of −500 to +4000 fs in 50 fs increments, at a fixed polarization geometry. At each position, in addition to recording the time dependent two-color photoelectron signal, the time invariant one-color pump alone and probe alone "background" signals were also sampled. At the end of each data collection run, the NO cross correlation was repeated in order to check for any drift in the position of time zero. This offset was typically less than 25 fs over 12 h of acquisition. Finally, switching the magnetic bottle into ion detection mode confirmed that no cluster formation occurred in the molecular beam expansion.

III. RESULTS AND DISCUSSION

A. "Time zero" photoelectron spectrum

Time resolved photoelectron spectra were recorded at pump wavelengths of 49 677 cm^{-1} (201.3 nm) and 50 075 cm^{-1} (199.7 nm), in each case chosen so as to sit between two strong vibrational bands in the $^1B_2(^1\Sigma_u^+)$ absorption spectrum, as summarized in Table I. At each wavelength, data were recorded with the angle between the polarization vector of the pump and probe beams set to 0° and 90° and the magic angle to 54.7°. We first summarize the key features of the spectra by presenting examples of the (200 and 267 nm one-color background subtracted) data obtained when the pump and probe pulses simply overlap in time. These are shown in Fig. 3. A strong vibrational progression
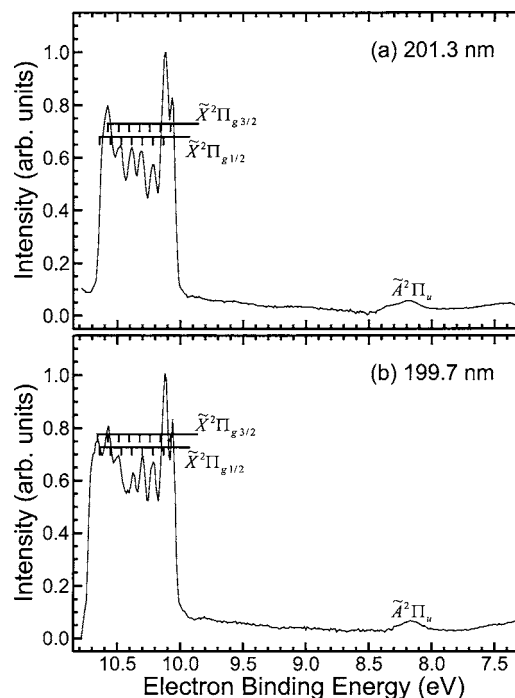
FIG. 3. Typical "background subtracted" two-color photoelectron spectrum of CS$_2$ obtained via the $\widetilde{X}\ ^1\Sigma_g^+ \rightarrow {}^1B_2(^1\Sigma_u^+)$ transition (a) at a central pump wavelength of 201.3 nm and a probe wavelength of 268.4 nm and (b) at a central pump wavelength of 199.7 nm and a probe wavelength of 266.3 nm. The combs approximate a progression in the symmetric stretch, ν_1^+, assuming a harmonic potential with a frequency of 655 cm^{-1} (81 meV) which is the average value of those reported in Refs. 42 and 43.

covers the 10.0–10.7 eV electron binding energy (E_b) range, terminating sharply at the total energy cutoff, one additional feature visible in the 199.7 nm pump wavelength spectrum compared with that obtained at 201.3 nm due to the slightly higher total available energy. No appreciable differences are observed in the appearance of the spectra as the angle between pump and probe polarizations is varied. The position of the lowest energy peak at 10.076±0.006 eV is in good agreement with the ionization potential (IP) value of 10.078 eV determined from a high resolution zero electron kinetic energy (ZEKE) measurement.[42] The separation between this peak and the one adjacent to it is 53±3 meV (430±25 cm^{-1}) which is close to a number of previously reported measurements of the spin-orbit splitting in the CS$_2^+$ ion of ~440 cm^{-1}.[42,43] We therefore assign the two lowest lying features in the spectra to ionization into the vibrational origins of the $\widetilde{X}\ ^2\Pi_{g3/2}$ and $\widetilde{X}\ ^2\Pi_{g1/2}$ spin-orbit states of CS$_2^+$. In the case of single photon ionization direct from the ground state of CS$_2$ these two peaks overwhelmingly dominate the appearance of the photoelectron spectrum in this energy region due to the essentially nonbonding character of the $2\pi_g$ orbital from which an electron is removed. The CS bond lengths are therefore very similar in the ground states of CS$_2$ and CS$_2^+$ (~1.55 Å in both instances[43,44]). On the basis of simple Franck-Condon arguments, "diagonal" transitions involving $\Delta\nu=0$ are therefore strongly favored. Since these transitions originate largely from the ground state vibrational origin (even at room temperature), the formation of higher lying ion vibrational states occurs with only very low
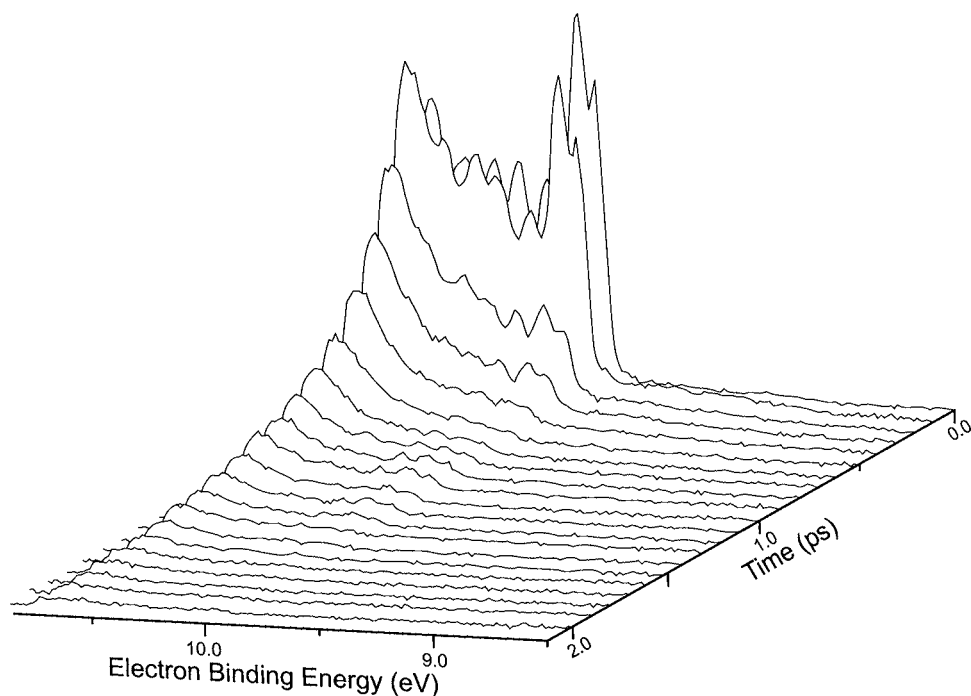
FIG. 4. Evolution of the $(1+1')$ CS_2 photoelectron spectrum as a function of pump-probe delay following excitation at 201.3 nm. For clarity, data are binned into 100 fs steps and only plotted out to 2 ps. The angle between pump and probe polarizations was set to 0° in this example.

propensity.[45–49] As already discussed in Sec. I, the $^1B_2(^1\Sigma_u^+) \leftarrow \widetilde{X}\,^1\Sigma_g^+$ transition promotes an electron from the $2\pi_g$ orbital to a $3\pi_u^*$ antibonding orbital and this extends the CS bond length to 1.66 A. Ionization proceeding via the intermediate $^1B_2(^1\Sigma_u^+)$ state would therefore be expected to give rise to a more extended vibrational progression in the electronic ground state of the CS_2^+ ion, and this indeed appears to be the case, as evidenced by the series of features at binding energies above 10.2 eV in Fig. 3. Owing to the inherent lack of spectral resolution in our time resolved experiment, a fully quantitative assignment is not possible. Based upon previously reported values of the vibrational frequencies in CS_2^+, however, a progression in the symmetric stretch, $\nu_1^+ \sim 655$ cm^{-1} (81 meV), seems to be a reasonable first approximation to the data,[42,43] as demonstrated by the combs overlaid on Fig. 3. The excitation energies of 49 677 and 50 075 cm^{-1} used in this study populate vibrational lines in the $^1B_2(^1\Sigma_u^+)$ state that are assigned as combinations of the symmetric stretch, ν_1', and the bending mode, ν_2'.[9] At these energies there is just enough energy available for the CS_2 molecule to overcome the small (~3500 cm^{-1}) potential barrier that exists along the bending coordinate and assume a quasilinear geometry.[9,12] A simple Franck-Condon analysis of a generic linear to bent transition in a triatomic molecule reveals that ν_2' excitation is expected to be strongest in the region close to the top of the barrier to linearity since the vibrational wave function in the upper state has large amplitude at bond angles close to 180° and therefore overlaps well with the $\nu_2'=0$ wave function in the linear ground state. At energies significantly above the barrier this is no longer the case as, within a classical picture, the upper state turning points become displaced to more acute S–C–S angles and the extent of the overlap is therefore considerably reduced. Such behavior has been well documented in previous studies of $^1B_2(^1\Sigma_u^+)$ absorption and emission in CS_2.[9,11,12] Similar arguments also govern the ionizing transition from the $^1B_2(^1\Sigma_u^+)$

state to the $\widetilde{X}\,^2\Pi_g$ state of CS_2^+. Vibrational states lying far above or below the barrier to linearity experience poor wave function overlap with the ν_2^+ levels of the linear ion, whereas those in close proximity to the barrier experience a strong propensity for the formation of $\nu_2^+=0$, once again as a consequence of the large vibrational wave function amplitude at bond angles close to 180°. Ionization of excited bending vibrations in the $^1B_2(^1\Sigma_u^+)$ state would therefore be expected to enhance the intensity of the photoelectron spectrum in the region of the ν_2^+ origin between 10.0 and 10.2 eV, as is indeed observed in Fig. 2. There is an additional possibility that nonresonant ionization (i.e., a "probe-pump" rather than a "pump-probe" signal) could also give rise to this enhancement since such a process would be expected to show strong spectral features in the same energy region (appearing similar to the photoelectron spectrum obtained directly from the ground state of CS_2). The very large ($f=1.1$) oscillator strength for CS_2 at ~200 nm strongly disfavors this process, however.

The two very weak features below 8.5 eV in Fig. 3 are due to higher order two-color processes involving absorption of more than two photons and therefore appear at binding energies that are seemingly lower than the ground state IP of the CS_2^+ cation. The position of the peak between 8.0 and 8.5 eV binding energy suggests that this is most likely (1 +2′) REMPI to the $\widetilde{A}\,^2\Pi_u$ state of CS_2^+ (IP=12.698 eV). The nature of the peak that appears just below 7.5 eV is unclear.

B. $^1B_2(^1\Sigma_u^+)$ state dynamics

Figure 4 displays the typical evolution of the photoelectron spectrum as a function of pump-probe delay. The most striking feature of this plot is that at binding energies greater than ~10.4 eV, the intensity of the photoelectron signal is clearly observed to rise in the first 100 fs before subsequently starting to decay, whereas at lower binding energies

this is not the case. This immediately provides a strong indication that the decay of the $^1B_2(^1\Sigma_u^+)$ state does not follow a simple monoexponential model and that a more sophisticated picture may be required to describe the dynamics.

As already outlined in Sec. I, previous time resolved studies of $^1B_2(^1\Sigma_u^+)$ state lifetimes monitored the total CS_2^+ ion yield as a function of pump-probe delay and modeled the decay dynamics using a single exponential fit to the data.[35,36] Time constants between 620 and 180 fs were reported, with faster decay rates correlating with increased excitation energy. The results of integrating our data (201.3 nm pump wavelength) over the 10.0–10.7 eV binding energy region (the total $1+1'$ signal) and performing a similar single exponential fit are shown in Fig. 5 for each of the three polarization schemes used. It is immediately apparent that the characteristics of the decaying signal change significantly as the polarization of the probe pulse is rotated relative to that of the pump and that, additionally, for all polarization geometries a single exponential model appears to yield an unsatisfactory fit. A very similar situation is also observed for excitation at 199.7 nm although the overall decay rates appear to be marginally faster. The pump wavelengths used in this study were chosen so as to simultaneously excite two vibrational lines in the $^1B_2(^1\Sigma_u^+)$ state absorption spectrum, in a manner akin to the work of Farmanara *et al.*[36] As discussed previously, these authors attributed deviations from a single exponential fit to quantum interference between the two coherently prepared vibrational levels, as evidenced by the close agreement between the reciprocal of the level spacing and the beating period observed in the residual signal (i.e., the fit subtracted from the experimental data). The residuals resulting from single exponential fits to our data are also shown in Fig. 5. We are unable to observe any clear regularity or "beating" in this signal, and this remains the case even when the fitting procedure is repeated with time zero artificially offset anywhere between ±50 fs (which is larger than any experimental drift we observe). Importantly, within a single decay channel model such as this, the modulation frequencies in the residual arising due to coherences between the two initially prepared states (in addition to the overall decay lifetime) must be invariant with respect to the probe polarization since the beat frequency only depends on the energy separation of the two states. This is not the case in our results. Finally, any beats observed in the total ion yield spectrum should appear even more prominently in the energy resolved TRPES. No clear signatures of quantum beating were observed in *any region of the photoelectron spectrum* when a global single exponential fit (i.e., simultaneously fitting to all electron energies) was performed on the (unintegrated) data.

An advantage of time resolved photoelectron spectroscopy over experiments monitoring only the evolution of the total ion yield is that, in cases where multiple decay pathways are present, the relative contribution of each component in a given (multiexponential) fit to the data may be examined independently as a function of electron kinetic energy. As will be seen, deconvoluting the photoelectron spectrum in this way greatly assists in the interpretation of the overall molecular dynamics.
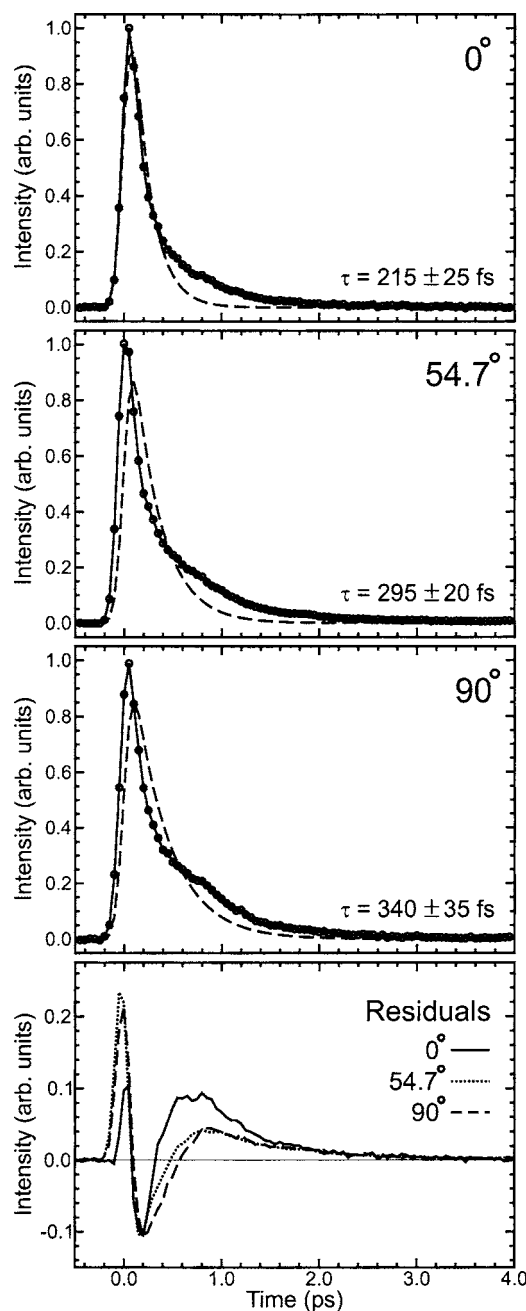
FIG. 5. Time dependence of the $(1+1')$ CS_2 photoelectron signal in the 10.0–10.7 eV binding energy region with the angle between pump and probe polarizations set to 0°, 54.7°, and 90°. The central pump wavelength was 201.3 nm. Also shown are single exponential fits to the data and the residuals from the fit. Note the change in the Y-axis scaling in the last plot.

In Fig. 6 we plot an example of the decay associated spectra that result from a Levenberg-Marquardt global biexponential fit over the 10.0–10.7 eV electron binding energy region. The corresponding lifetimes associated with each decay channel are summarized in Table II and the data, overall fit, and associated residual are plotted in Fig. 7. At all electron energies, the quality of the fit is greatly improved over the single exponential case, with the data exhibiting a clear "fast" component τ_1 of $\leqslant 50$ fs and a "slow" component τ_2 rising from 510 to 640 fs at an excitation wavelength of 201.3 nm (from 360 to 480 fs at 199.7 nm) as the angle between pump and probe polarizations is increased from 0° to
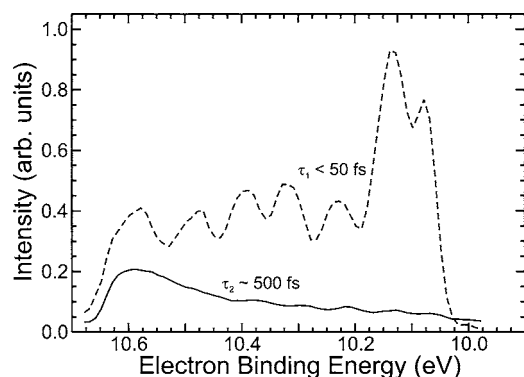
FIG. 6. Decay associated spectra for the fast and slow components of a two exponential fit to the time dependent CS_2 photoelectron signal at a pump wavelength of 201.3 nm. The angle between pump and probe polarizations is 0°. Both exponentials originate from t_0 (parallel mechanism).

TABLE II. Time constants obtained from a global biexponential fit to time resolved photoelectron spectra of CS_2 obtained at different pump wavelengths and pump-probe polarization angles.

λ_{pump}		$^1\Sigma_u^+(^1B_2)$ state lifetime (fs)		
		0°	54.7°	90°
49 677 cm^{-1} (201.3 nm)	τ_1	45±20	35±15	25±15
	τ_2	510±30	610±25	640±30
50 075 cm^{-1} (199.7 nm)	τ_1	45±25	30±15	20±10
	τ_2	360±35	415±25	480±40

90°. The relative amplitudes of the two components in the fit were not observed to change significantly with polarization. Given an experimental cross correlation of ~160 fs, any values explicitly quoted for τ_1 have large error bars and hence we assign the fast component to be nominally ≲50 fs in all cases, making no clear distinction between different polarization schemes and/or excitation wavelengths. Note that in Fig. 6, the amplitudes of the decay associated spectra are nonzero for both channels over the entire 10.0–10.7 eV region, although the relative contribution changes considerably, with the slow decay pathway becoming more pronounced at higher binding energies. On the basis of the photoelectron spectrum assignment presented in the previous section, this would seem to imply that the excited CS_2 molecule has a higher propensity to dissociate via the fast pathway at more bent geometries, whereas the slower channel tends to play an increased role in linear configurations.

Although a parallel biexponential model provides a reasonably good fit to the data, the considerable variation of τ_2 with pump-probe polarization angle reveals a more complex picture of the underlying dynamics in the $^1B_2(^1\Sigma_u^+)$ state of CS_2 than this straightforward two pathway picture initially suggests. For the case of a single initially prepared state decaying to a single final state, the observed lifetime is expected to be independent of polarization, even though the overall ionization cross section (i.e., the observed photoelectron signal level) may change considerably. We therefore take the apparent polarization dependence of the slow component lifetime to indicate the presence of multiple initial and/or final states contributing to this decaying signal. The relative changes in ionization cross section for these various states at different polarization geometries may therefore give rise to a variation in the experimentally observed lifetime. This lifetime in effect represents a weighted average of all contributing channels in a given pump-probe polarization scheme. This is not an unreasonable assertion in this instance since we are populating multiple vibrational states in the initial excitation step, and additionally, from the photodissociation studies described previously, it is known that each of these may ultimately dissociate to either singlet or triplet products.

On the basis of the data presented here and in previous studies, we suggest the following model to explain our experimental observations. Firstly, the fast (<50 fs) channel most likely is the result of hot band transitions originating from $\nu_2''=1$ in the ground state and correlating with $K'=1$ in the bent $^1B_2(^1\Sigma_u^+)$ state, as discussed in the Introduction. In lower energy regions of the absorption and PHOFEX spectra,[13,33,34] both Σ- and Π-type resonant transitions are observed, although the lifetime associated with the latter is considerably shorter. This observation was attributed to an increased coupling rate to the dissociative asymmetric stretching coordinate through a Coriolis interaction. At higher excitation energies (such as those used in the present study) no Π transitions were observed, presumably since the rate of predissociation becomes so rapid (i.e., <50 fs according to our fit) that the line broadens into the base line (giving rise to the observed "continuum background"). Since we are unable to characterize the temperature of the molecular beam used in our experiment and, additionally, since we employ a continuous rather than a pulsed source, this explanation seems plausible. Some supporting evidence for this assertion comes from the fact than in limited preliminary data recorded using a 250 μm diameter nozzle (rather than the 150 μm diameter used for the vast majority of the work outlined here) the amplitude of the fast channel relative to the slow channel obtained from a biexponential fit was seen to increase, possibly as a result of the milder expansion conditions and hence warmer beam (and a greater proportion of associated hot band contributions to the overall absorption). Differences in molecular beam vibrational temperature also offer a possible explanation for the differences observed in the single exponential fit presented by Farmanara *et al.* and our energy integrated data in Fig. 5. Changes in the relative contributions of the fast and slow channels may excerpt considerable influence over the appearance of the decaying pump-probe signal and the associated fit and residuals.

Ionization of these very short lived states effectively establishes a rapidly moving "Franck-Condon window" that significantly shifts the appearance of the photoelectron spectrum over the first 100 fs, as is indeed observed. At zero time delay between pump and probe lasers, ionization is predominantly into the ground state modes of the CS_2^+ cation. As the wave packet (rapidly) exits the Franck-Condon region for the initial excitation step, Franck-Condon factors for the ionization step begin to favor population of higher lying CS_2^+ vibrational states. This has the effect of shifting the component of the photoelectron spectrum arising from the fast channel
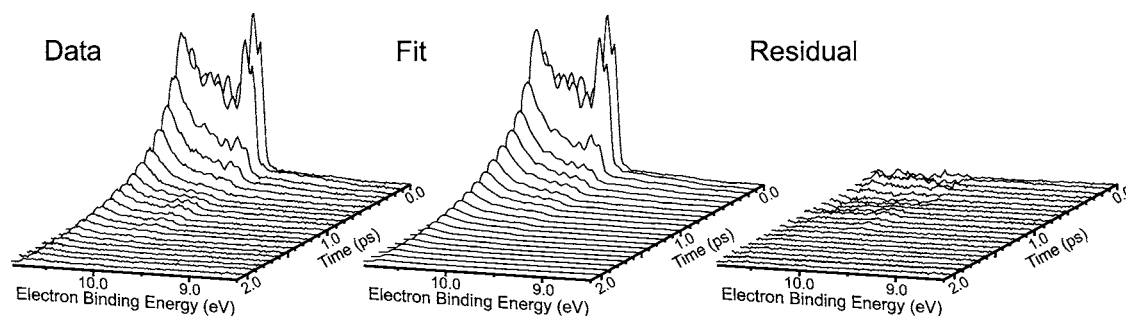
FIG. 7. Time evolution of a CS$_2$ photoelectron spectrum is shown along with the results of a global biexponential fit and the associated residual plot. The pump wavelength is 201.3 nm and the angle between pump and probe polarizations is 0° in this instance.

to larger binding energies, creating an apparent rise in the observed signal, as is seen in Fig. 4. At pump-probe delays longer than ~100 fs (but probably less than 200 fs, by which time the molecule is likely to be fully fragmented) the SC–S bond has elongated sufficiently to move the Franck-Condon window into a region that is not energetically accessible at the ~267 nm probe wavelength.

We note that a second possibility for the origin of the fast channel is that of direct excitation to a different, purely dissociative state lying close in energy to $^1B_2(^1\Sigma_u^+)$. Possible candidates for this are the $^3\Sigma_g^-$ and $^3\Pi_g$ states, which are expected to lie in a similar energy region,[34] although in the absence of any detailed potential energy surface calculations this is somewhat speculative. This picture is also consistent with the observation of sharp resonances superimposed on top of a weak continuum signal [particularly in the S(^3P) channel] reported in the PHOFEX spectra. Owing to the large (400 cm^{-1} FWHM) bandwidth of the femtosecond pump pulses in our experiment [the maximum intensity of which is positioned *between* two of these resonant (~15 cm^{-1} FWHM) features], this magnitude of the off-resonant signal becomes significant with respect to the resonant excitation to the $^1B_2(^1\Sigma_u^+)$ state, as evidenced by the decay associated spectra in Fig. 6. Although a singlet-triplet transition such as this is formally forbidden, spin-orbit coupling induced by the relatively heavy sulfur atoms would be expected to result in a breakdown of this restriction.

The origin of the slow channel would seem to be consistent with excitation to $K'=0$ levels of the $^1B_2(^1\Sigma_u^+)$ state and subsequent dissociation along the SC–S antisymmetric stretching coordinate to form S(^1D) or S(^3P) products. As previously suggested by Mank *et al.*, surface crossing to the nearby $^3\Sigma_g^-$ and/or $^3\Pi_g$ triplet states due to the relatively strong spin-orbit coupling interaction in CS$_2$ leading to triplet products seems likely to occur along this reaction coordinate. From inspection of the PHOFEX spectra reported for the S(^1D) and S(^3P) products, the lifetimes of these two pathways appear to be similar (based upon a comparison of the linewidths). Unfortunately, detailed analysis of the lifetimes for the individual channels was not reported. It seems reasonable, however, to expect some differences in the lifetimes of the two dissociation pathways. The dependence of the experimentally determined lifetime we observe for the slow channel as a function of the angle between pump and probe laser polarizations is therefore a consequence of changes in the differential ionization cross section of the $^1B_2(^1\Sigma_u^+)$ state relative to the $^3\Sigma_g^-/^3\Pi_g$ states.

The involvement of distinct *electronic* states contributing to the slow channel is strongly indicated by the fact that for all polarization schemes used, the appearance of the vibrational structure in the photoelectron spectrum always remains invariant. In the event that changes to the observed lifetime with polarization in the slow channel were the result of changes in the differential ionization cross sections of the various states composing the initially prepared vibrational wave packet, this observation would seem unlikely. Evolution of the character of the electronic wave function as the CS$_2$ molecule dissociates into CS+S(^3P) products therefore implies that the set of photoelectron partial waves associated with the formation of the ground electronic state of the CS$_2^+$ cation will also evolve accordingly. Observation and subsequent analysis of the photoelectron angular distribution as a function of pump-probe delay would therefore provide a more differential measurement of the decay dynamics and, on the basis of symmetry arguments, provide a route to the unambiguous determination of which triplet state is involved. Efforts to carry out such experiments are currently under way in our group.

Owing to the inherent difficulties associated with reliably fitting two time constants within the same decade, we are unable to extract separate lifetimes for these two individual components directly from the data (using either a parallel or a sequential model). In addition, in the absence of any knowledge relating to the differential ionization cross sections of the two electronic states, we are unable to obtain distinct lifetimes for the singlet and triplet channels by deconvoluting the data obtained over a range of pump-probe polarization angles.

Averaging the time constants extracted for the long channel over the three polarization geometries used yields lifetimes of 420 and 585 fs for excitations at 199.7 and 201.3 nm, respectively. These values are in excellent agreement with the lifetimes reported in the PHOFEX measurements for the resonant lines excited in these regions (which do not include any significant contributions from the fast continuum background). We note, however, that this is a somewhat crude comparison since our average is not weighted by the total ionization cross section at each polarization angle (which we are unable to extract from our data).

In conclusion, through the use of femtosecond TRPES we have been able to deconvolute the decay dynamics of the $^1B_2(^1\Sigma_u^+)$ state of CS_2. Decay of the molecule occurs on two distinct time scales, the longer of which clearly involves coupling to a second excited electronic state prior to dissociation, consistent with previous interpretations of the dynamics. The origin of the fast channel is most likely due to hot band transitions originating from the vibrationally excited ground state and correlating with $K'=1$ in the bent $^1B_2(^1\Sigma_u^+)$ state. At pump energies sufficient to enable the electronically excited CS_2 molecule to assume a quasilinear geometry, these $K'=1$ levels are able to couple to the dissociative asymmetric stretching coordinate almost instantaneously.

ACKNOWLEDGMENTS

[1] The $^1\Sigma_u^+(^1B_2)$ state is in some cases more completely denoted as $\widetilde{C}\ ^1B_2(^1\Sigma_u^+)$ (which is consistent with the alternative S_3 label) although there is some inconsistency as a number of authors have used $\widetilde{A}\ ^1B_2(^1\Sigma_u^+)$ or even refer simply to the $\widetilde{A}$ state when describing the 185–230 nm absorption band. This would seem to be incorrect since there are two well documented lower lying singlet absorption bands of CS_2, in the 290–330 nm ($^1\Delta_u$) and 330–390 nm ($^1\Sigma_u^-$) regions [see J. W. Rabalais *et al.*, Chem. Rev. (Washington, D.C.) **71**, 73 (1971) for more information]. The $\widetilde{C}$ label has also been used to refer to the upper ($^1A_2$) Renner-Teller component derived from the $^1\Delta_u$ state in bent geometries [see Q. Zhang and P. H. Vaccaro, J. Phys. Chem. **99**, 1799 (1995) for more details]. To avoid further confusion, and in keeping with the notation used in most other studies of the 185–230 nm absorption band, we shall omit this prefix altogether.

[2] R. S. Mulliken, J. Chem. Phys. **7**, 20 (1939).

[3] A. D. Walsh, J. Chem. Soc. **1953**, 2260.

[4] R. S. Mulliken, Can. J. Chem. **36**, 10 (1958).

[5] A. E. Douglas and I. Zanon, Can. J. Phys. **42**, 627 (1964).

[6] S. C. Yang, A. Freedman, M. Kawasaki, and R. Bersohn, J. Chem. Phys. **72**, 4058 (1980).

[7] W. C. Price and D. M. Simpson, Proc. R. Soc. London, Ser. A **165**, 272 (1938).

[8] K. Hara and D. Phillips, J. Chem. Soc., Faraday Trans. 2 **74**, 1441 (1978).

[9] R. J. Hemley, D. G. Leopold, J. L. Roebber, and V. Vaida, J. Chem. Phys. **79**, 5219 (1983).

[10] J. L. Roebber and V. Vaida, J. Chem. Phys. **83**, 2748 (1985).

[11] D. J. Donaldson, J. Chem. Phys. **91**, 7455 (1989).

[12] M. F. Arendt and L. J. Butler, J. Chem. Phys. **109**, 7835 (1998).

[13] A. S. Beatty, R. C. Shiell, D. Chang, and J. W. Hepburn, J. Chem. Phys. **110**, 8476 (1999).

[14] R. R. Sadeghi, S. R. Gwaltney, J. L. Krause, R. T. Skodje, and P. M. Weber, J. Chem. Phys. **107**, 6570 (1997).

[15] As mentioned in the main text, the labels Σ_0 and Π_1 are used to denote transitions originating from $\nu_2''=0$ and $\nu_2''=1$ in the ground state, respectively (as denoted by the "0" and "1" subscripts). The Σ, Π, Δ, etc., labels indicate the ground state vibrational angular momentum (which is directed along the internuclear axis), corresponding to $l=0,1,2,\ldots$, respectively. These states may also be labeled $(0, 0^0, 0)$ and $(0, 1^1, 0)$ in a more conventional (ν_1, ν_2^l, ν_3) scheme. Note that since ν_2'' is the only degenerate vibration in the linear CS_2 molecule, it is the only one with associated angular momentum. Note also that the 0 and 1 labels are sometimes dropped in vibrationally cold experiments where there is no significant population in $\nu_2''=2$ (where a distinction between, for example, Σ_0 and Σ_2 is not required).

[16] Angular momentum selection rules governing parallel linear-bent transitions (where the bent state is a near prolate symmetric top with rotational constants $A>B\approx C$, as is the case in CS_2) state that $\Delta K=K'-K''=0$. For a linear $^1\Sigma$ electronic state ($\Lambda=0$), K'' (the projection of the total angular momentum onto the principal symmetry axis) is simply equal to l. In a bent configuration, l is not well defined and K' represents the projection of total electronic (when $\Lambda\neq0$), vibrational, and rotational angular momenta. Transitions from $\nu_2''=0$ therefore correlate with $K'=0$ (Σ_0 transitions) and those from $\nu_2''=1$ correlate with $K'=1$ (labeled Π_1). Transitions such as Π_0 do not exist.

[17] B. Li and A. B. Meyers, J. Chem. Phys. **94**, 2458 (1991).

[18] H. T. Liou, P. Dan, T. Y. Hsu, H. Yang, and H. M. Lin, Chem. Phys. Lett. **192**, 560 (1992).

[19] J. E. Butler, W. S. Drozdoski, and J. R. McDonald, Chem. Phys. **50**, 413 (1980).

[20] V. R. McCrary, R. Lu, D. Zakheim, J. A. Russell, J. B. Halpern, and W. M. Jackson, J. Chem. Phys. **83**, 3481 (1985).

[21] I. M. Waller and J. W. Hepburn, J. Chem. Phys. **87**, 3261 (1987).

[22] W.-B. Tzeng, H.-M. Yin, W.-Y. Leung, J.-Y. Luo, S. Nourbakhsh, G. D. Flesch, and C. Y. Ng, J. Chem. Phys. **88**, 1658 (1988).

[23] S. M. McGivern, O. Sorkhabi, A. H. Rizvi, A. G. Suits, and S. W. North, J. Chem. Phys. **112**, 5301 (2000).

[24] T. N. Kitsopoulos, C. R. Gebhardt, and T. P. Rakitzis, J. Chem. Phys. **115**, 9727 (2001).

[25] H. Kanamori and E. Hirota, J. Chem. Phys. **86**, 3901 (1987).

[26] M. C. Addison, R. J. Donovan, and C. Fotakis, Chem. Phys. Lett. **74**, 58 (1980).

[27] G. Dornhofer, W. Hack, and W. Langel, J. Phys. Chem. **88**, 3060 (1984).

[28] G. Black and L. E. Jusinski, Chem. Phys. Lett. **124**, 90 (1986).

[29] D. Xu, J. Huang, and W. M. Jackson, J. Chem. Phys. **120**, 3051 (2004).

[30] J. G. Frey and P. Felder, Chem. Phys. **202**, 397 (1996).

[31] H. T. Liou, K. L. Huang, and M. C. Chen, Chem. Phys. Lett. **266**, 591 (1997).

[32] H. T. Liou, Y. C. Chang, K. L. Huang, and W. C. Lin, J. Phys. Chem. A **101**, 6723 (1997).

[33] C. Starrs, M. N. Jego, A. Mank, and J. W. Hepburn, J. Phys. Chem. **96**, 6526 (1992).

[34] A. Mank, C. Starrs, M. N. Jego, and J. W. Hepburn, J. Chem. Phys. **104**, 3609 (1996).

[35] A. P. Baronavski and J. C. Owrutsky, Chem. Phys. Lett. **221**, 419 (1994).

[36] P. Farmanara, V. Stert, and W. Radloff, J. Chem. Phys. **111**, 5338 (1999).

[37] V. Blanchet, M. Z. Zgierski, T. Seideman, and A. Stolow, Nature (London) **401**, 52 (1999).

[38] A. Stolow, A. E. Bragg, and D. M. Neumark, Chem. Rev. (Washington, D.C.) **104**, 1719 (2004).

[39] A. Stolow, Annu. Rev. Phys. Chem. **54**, 89 (2003).

[40] P. Kruit and F. H. Read, J. Phys. E **16**, 313 (1983).

[41] S. Lochbrunner, J. J. Larsen, J. P. Shaffer, M. Schmitt, T. Schultz, J. G. Underwood, and A. Stolow, J. Electron Spectrosc. Relat. Phenom. **112**, 183 (2000).

[42] I. Fischer, A. Lochschmidt, A. Strobel, G. Niedner-Schattebrug, K. Muller-Dethlefs, and V. E. Bondybey, Chem. Phys. Lett. **202**, 542 (1993) and references cited therein.

[43] S.-G. He and D. J. Clouthier, J. Chem. Phys. **124**, 084312 (2006).

[44] D. S. Kummli, H. M. Frey, and S. Leutwyler, J. Chem. Phys. **124**, 144307 (2006).

[45] J. W. Rabalais, *Principles of Ultraviolet Photoelectron Spectroscopy* (Wiley-Interscience, New York, 1977) and references cited therein.

[46] R. Frey, B. Gotchev, W. B. Peatman, H. Pollak, and E. W. Schlag, Int. J. Mass Spectrom. Ion Phys. **26**, 137 (1978).

[47] M.-J. Hubin-Franskin, J. Delwiche, P. Natalis, G. Caprace, and D. Roy, J. Electron Spectrosc. Relat. Phenom. **18**, 295 (1980).

[48] I. Reineck, B. Wannberg, H. Veenhuizen, C. Nohre, R. Maripuu, K.-E. Norell, L. Mattsson, L. Karlsson, and K. Siegbahn, J. Electron Spectrosc. Relat. Phenom. **34**, 235 (1984).

[49] L.-S. Wang, J. E. Reutt, Y. T. Lee, and D. A. Shirley, J. Electron Spectrosc. Relat. Phenom. **47**, 167 (1988).

[50] B. Li, A. B. Meyers, and X. Ci, J. Chem. Phys. **89**, 1876 (1988).

[51] B. Li and A. B. Meyers, J. Chem. Phys. **89**, 6658 (1988).